PHYSICAL REVIEW E VOLUME 62, NUMBER 5 NOVEMBER 2000

Nonlinear dielectric relaxation spectroscopy of ferroelectric liquid crystals

Yasuyuki Kimura, Shun Hara, and Reinosuke Hayakawa
Department of Applied Physics, Graduate School of Engineering, University of Tokyo, 7-3-1 Hongo, Bunkyo-Ku, Tokyo 113-8656, Japan
(Received 1 February 2000)

The nonlinear dielectric relaxation spectra of ferroelectric liquid crystals (FLCs) have been studied in the chiral smectic-*C* phase. The linear and third-order nonlinear dielectric spectra show the relaxation corresponding to the fluctuation in the azimuthal angle of directors called the Goldstone mode. We calculated the nonlinear dielectric spectra of the Goldstone mode theoretically by the torque balance equation which describes the dynamics of FLCs under the electric field. The calculated spectra make good agreement with the measured ones. We also evaluated the material constants of FLCs from the best-fitted values of the linear and nonlinear dielectric increment and relaxation time.

PACS number(s): 61.30.Gd, 77.22.Gm, 77.84.−s, 05.45.−a

Ferroelectric liquid crystals (FLCs) have attracted much attention of researchers from the fundamental and technological points of view since the discovery of the ferroelectricity in the chiral smectic-*C* (Sm-*C**) phase [1]. In the Sm-*C** phase, the constituent chiral molecules tilt from the layer normal and form a helical structure whose axis is parallel to the layer normal. The spontaneous polarization lies in the plane of the smectic layers and is perpendicular to the long molecular axis (director). In the lower frequency region below several MHz, there are two collective fluctuation of the directors in the Sm-*C** phase [2]. One is the soft (amplitude) mode, which is the fluctuation in the magnitude of the tilt angle. The other is the Goldstone (phase) mode, which is the fluctuation in the azimuthal angle of director around the helical axis. They have been intensively studied theoretically and experimentally, especially by the dielectric relaxation spectroscopy [3–8]. As the dielectric increment and relaxation time of the Goldstone mode is usually large, this mode is predominant in the dielectric response in the Sm-*C** phase except at the vicinity of the Sm-*A*–Sm-*C** phase transition temperature.

In soft materials such as liquid crystals and polymers, their response to external field is expected to become easily nonlinear even under the small applied field. Recently, the dielectric relaxation spectroscopy has been extended to the nonlinear regime and applied to research on polymers [9–11] and liquid crystals [12–14]. In these studies, it is shown that the nonlinear spectra offer more information on the dynamics of molecules and the phase transition than that obtained only by the linear spectrum.

In this Rapid Communication, we have applied the nonlinear dielectric relaxation spectroscopy to the Goldstone mode of FLCs in the Sm-*C** phase and analyzed the obtained spectra by those calculated theoretically. We also discuss the availability of the nonlinear dielectric relaxation spectroscopy to the measurement of material constants of FLCs in thick samples.

We can discuss the dynamics of the azimuthal angle of director $\varphi(z,t)$ around the helical axis (taken as the z axis) under the electric field E with the amplitude E_0 and the angular frequency ω, $E=E_0\cos\omega t$, applied parallel to the y axis by the torque balance equation in the constant amplitude approximation [6],

$$K\frac{\partial^2\varphi}{\partial z^2}-\gamma\frac{\partial\varphi}{\partial t}=P_S E\sin\varphi, \tag{1}$$

where $K\equiv K_3\sin^2\theta$, $\gamma\equiv\gamma_0\sin^2\theta$, K_3 is the elastic constant, γ_0 is the rotational viscosity, θ is the tilt angle, and P_S is the spontaneous polarization. If the applied field is very small, the solution of Eq. (1) is written in the perturbed form to the solution for $E_0=0$, $\varphi_0(z)=q_0z$, where q_0 is the wave number of the helical structure. We assume that the tilt angle and the helical pitch will not change under the small electric field we used, and the boundary condition for $\varphi_0(z)$ is also applicable to $\varphi(z,t)$. Then, the solution of Eq. (1) is written as a sum of the fundamental and harmonic components of ω and their amplitudes are expanded into the power series of E_0 and the Fourier series of $\sin(mq_0z)$ $(m=1,2,\ldots)$,

$$\varphi(z,t)=q_0z+\sum_{n=1}^{\infty}\sum_{m=1}^{\infty}\sum_{r=0}^{n}A_{nmr}\left(\frac{E_0}{2}\right)^n \times e^{i(n-2r)\omega t}\sin(mq_0z). \tag{2}$$

By replacing $\varphi(z,t)$ in Eq. (1) with Eq. (2), we can determine all coefficients A_{nmr} in Eq. (2).

The polarization induced parallel to the applied electric field E is calculated by averaging $P_S\cos\varphi$ over one helical pitch. We finally obtain the induced electric displacement D for the Goldstone mode as a sum of the fundamental and harmonic components of ω,

$$D(t)=2\sum_{m=1}^{\infty}\mathrm{Re}[D_m^*e^{im\omega t}] =2\sum_{m=1}^{\infty}\sum_{r=0}^{\infty}\mathrm{Re}[\varepsilon_{m,m+2r}^*e^{im\omega t}]\left(\frac{E_0}{2}\right)^{m+2r}, \tag{3}$$

where D_m^* is the complex amplitude of the mth-order harmonic component and ε_{mn}^* is the complex nonlinear dielectric constant defined as the coefficient of the term proportional to $(E_0/2)^n$ in D_m^*. The even-order harmonic components disappear by the symmetry of polarization. When the applied field E_0 is small, the dominant term in D_m^*

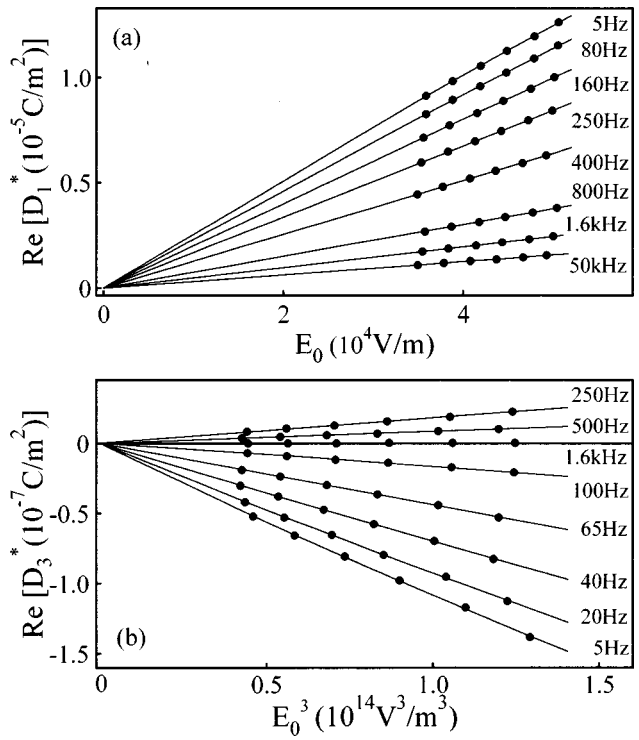

FIG. 1. Applied electric field E_0 dependence of the real part of (a) D_1^* and (b) D_3^* of CS1017 for several frequencies at 50 °C. The solid lines in (a) are the best-fitted lines of $D_1^*=\varepsilon_1^* E_0$. The solid lines in (b) are the best-fitted lines of $D_3^*=\varepsilon_3^* E_0^3/4$.

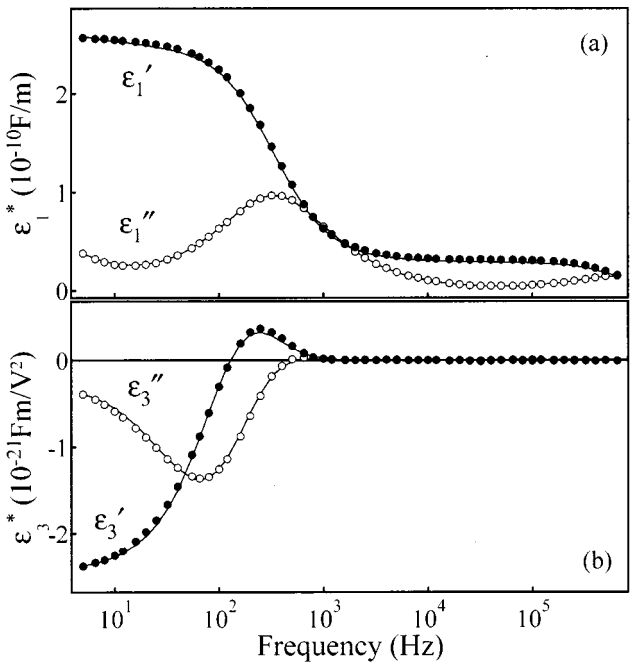

FIG. 2. (a) Linear ε_1^* and (b) the third-order nonlinear dielectric relaxation spectrum ε_3^* of CS1017 at 50 °C. The solid line in (a) is the best-fitted curve of the modified form of Eq. (7) in which the effect of the resistance of ITO electrodes is considered. The solid line in (b) is the best-fitted curve of Eq. (8).

is that proportional to E_0^m. We can experimentally obtain the mth-order nonlinear dielectric spectrum ε_m^* ($\equiv\varepsilon_{mm}^*$) from the applied field E_0 dependence of D_m^* as

$$\varepsilon_m^* = \lim_{E_0\to 0} \frac{D_m^*}{E_0^m}\cdot 2^{m-1} \equiv \varepsilon_m' - i\varepsilon_m''. \tag{4}$$

We can obtain the linear ε_1^* and third-order nonlinear dielectric spectrum ε_3^* of the Goldstone mode from Eqs. (3) and (4) as [15,16]

$$\varepsilon_1^* = \frac{P_S^2}{2Kq_0^2}\cdot\frac{1}{1+i\omega\tau}, \tag{5}$$

$$\varepsilon_3^* = -\frac{P_S^4}{16(Kq_0^2)^3}\cdot\frac{3+5i\omega\tau-\omega^2\tau^2}{(1+i\omega\tau)^3(1+i\omega\tau/2)(1+3i\omega\tau)}, \tag{6}$$

where τ is the relaxation time of the linear spectrum defined as $\tau=\gamma/Kq_0^2$. The negative increment of ε_3^* indicates that the nonlinear dielectric response of the Goldstone mode of FLCs originates from the saturation in the orientation of spontaneous polarization by the applied electric field. This is similar to the nonlinear dielectric response of the freely rotatable dipole moments [17].

The sinusoidal electric field $E(t)$ generated from the synthesizer (HP3326A) in the frequency range from 5 Hz to 800 kHz is applied to the sample after passing through the low pass filter (NF3656) to reduce the harmonic distortions in $E(t)$. The electric displacement $D(t)$ detected by a charge amplifier was digitized and transformed into complex spectrum data on the vector signal analyzer (HP89401A). The advantage of the nonlinear dielectric relaxation spectroscopy in the frequency-domain is to enable us to separate the nonlinear responses as harmonic components from the linear one by their frequencies. We have measured the applied electric field E_0 dependence of the complex amplitudes of the fundamental, second-order and third-order harmonic components of $D(t)$, D_1^*, D_2^*, and D_3^*.

The sample used in this study was mixture FLC, CS1017 (Chisso), and was sandwiched between two glass plates with indium tin oxide (ITO) electrodes. The surfaces of the cell were spin-coated with polyimide and rubbed unidirectionally to attain homogeneous alignment of molecules. The cell thickness was 25 μm, which was determined by the capacitance of the empty cell.

The typical dependence of the real part of D_1^* and D_3^* on the applied electric field E_0 in the Sm-C^* phase (50.0 °C) are respectively shown in Fig. 1. It is found that D_1^* and D_3^* have the linear relations to E_0 and E_0^3 respectively, but D_2^* is negligibly small compared to D_3^* within the range of E_0 we used. The linear and third-order nonlinear dielectric spectra ε_1^* and ε_3^* obtained by Eq. (4) are shown in Fig. 2.

The linear spectrum ε_1^* shows two relaxation of Debye type at about 300 Hz and 650 kHz. The relaxation in the higher frequency region is due to the series circuit made up of the resistance of ITO electrodes and the capacitance of the sample cell at high frequencies. The relaxation in the lower frequency region is that of the Goldstone mode and its spectrum can be well ascribable by the modified form of Eq. (5) with the distribution of relaxation times represented by the Cole-Cole parameter β_1 as

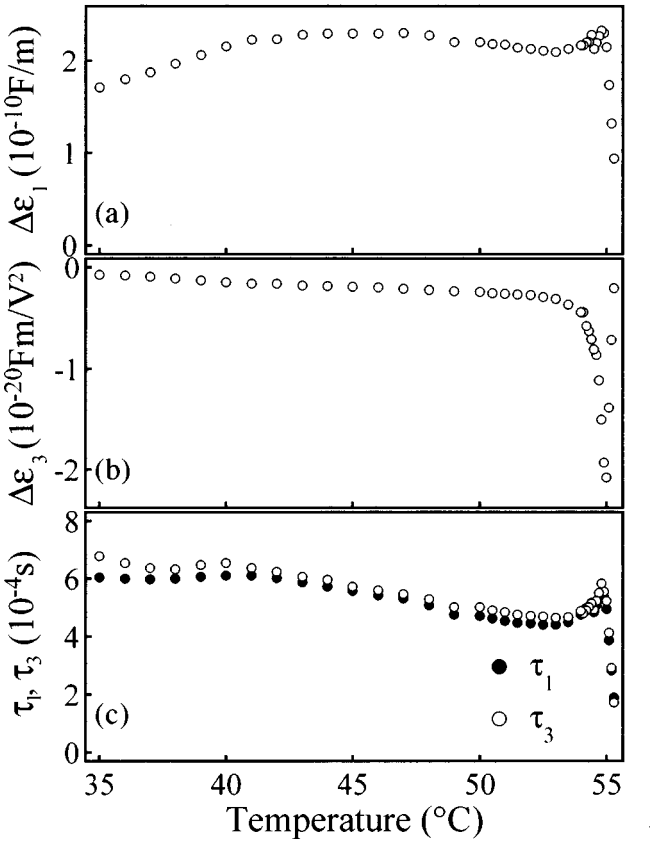

FIG. 3. Temperature dependence of the best-fitted parameters (a) $\Delta\varepsilon_1$, (b) $\Delta\varepsilon_3$ and (c) relaxation time τ_1 (●) and τ_3 (○) obtained using Eqs. (7) and (8) for ε_1^* and ε_3^*.

$$\varepsilon_1^* = \varepsilon_\infty + \frac{\Delta\varepsilon_1}{1+(i\omega\tau_1)^{\beta_1}} + \frac{A}{(i\omega)^{\gamma_1}}, \tag{7}$$

where $\Delta\varepsilon_1$ is the linear dielectric increment, τ_1 is the linear relaxation time, and ε_∞ is the permittivity at sufficiently high frequencies. For the better fitting of the data at low frequencies, we add the last term on the right-hand side of Eq. (7), which represents the effects of conductivity and electrode polarization. If we set γ_1 to unity, the parameter A reduces to the dc conductivity of the sample. The best-fitted curve in which the influence of the resistance of ITO electrodes is also introduced to Eq. (7) with $\tau_1 = 0.47$ ms, $\beta_1 = 0.91$, and $A/(i\omega)^{\gamma_1} = 5.6\times10^{-10}/(i\omega)^{0.81}$ F/m is drawn as a solid line in Fig. 2(a).

The third-order nonlinear spectrum ε_3^* shows the single relaxation corresponding to the Goldstone mode and has negative increment. Its profile can be well ascribable by the modified form of Eq. (6) as

$$\varepsilon_3^* = \frac{\Delta\varepsilon_3\{1+5(i\omega\tau_3)^{\beta_3}/3+(i\omega\tau_3)^{2\beta_3}/3\}}{\{1+(i\omega\tau_3)^{\beta_3}\}^3\{1+(i\omega\tau_3)^{\beta_3}/2\}\{1+3(i\omega\tau_3)^{\beta_3}\}} + \frac{B}{(i\omega)^{\gamma_3}}, \tag{8}$$

where $\Delta\varepsilon_3$, τ_3, and β_3 are respectively the third-order nonlinear dielectric increment, relaxation time, and Cole-Cole parameter. The second term on the right-hand side of Eq. (8) is necessary to fit the experimental data at low frequencies better. The best-fitted curve of Eq. (8) with $\tau_3 = 0.49$ ms, $\beta_3 = 0.89$, and $B/(i\omega)^{\gamma_3} = -5.4\times10^{-24}/(i\omega)^{0.89}$ Fm/V^2 is drawn as a solid line in Fig. 2(b). The best-fitted values of τ_i and β_i $(i=1,3)$ do not strongly depend on i, which confirms the theoretical prediction that the profiles of the nonlinear spectra are determined by the relaxation time of the linear spectrum τ_1.

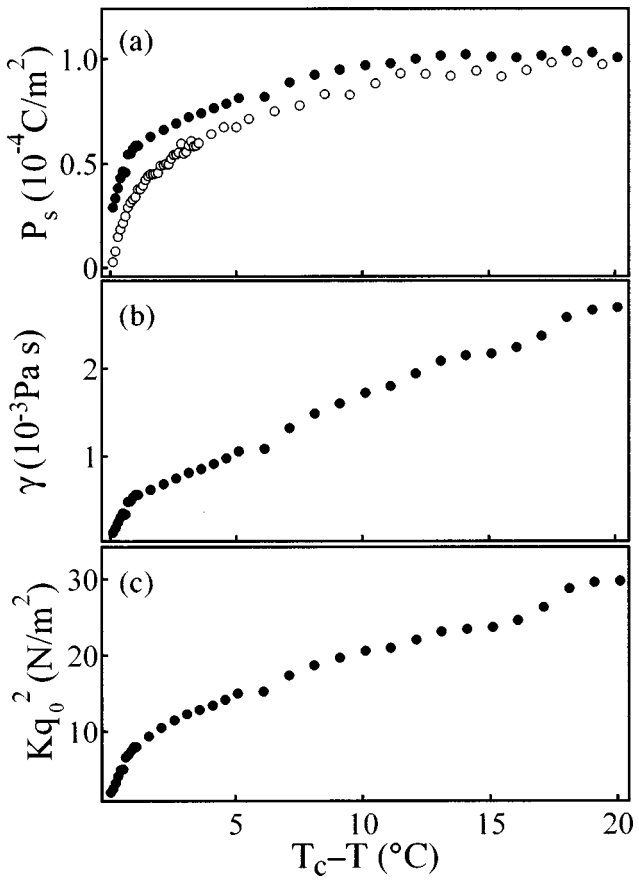

FIG. 4. Temperature dependence of (a) spontaneous polarization P_S, (b) rotational viscosity γ, and (c) Kq_0^2 calculated by Eqs. (9)–(11). The open circles in (a) are the values of P_S measured by the triangular wave method with the electric field of 1.6 MV/m and 20 Hz.

The temperature dependence of the best-fitted values of $\Delta\varepsilon_1$, $\Delta\varepsilon_3$, τ_1, and τ_3 are shown in Fig. 3. The increment $\Delta\varepsilon_1$ shows a small peak just below the Sm-A–Sm-C^* phase transition temperature T_C and takes an almost constant value except that region. The magnitude of $\Delta\varepsilon_3$ also takes a maximum value near T_C and decreases rapidly with decreasing temperature in the Sm-C^* phase. The observed values of $\Delta\varepsilon_3$ are four or more decades larger than those reported for ferroelectric or polar polymers in magnitude [9–11]. In FLCs, the helical structure with a long pitch brings about a large fluctuation of dipole moments. Hence, a small electric field can easily deform the helical structure which results in a large nonlinear permittivity of FLCs. The relaxation times τ_1 and τ_3 take almost same values with the ratio τ_3/τ_1 of 1.05 and their temperature dependence are almost same as that of $\Delta\varepsilon_1$. The observed temperature dependence of $\Delta\varepsilon_1$ and τ_1 are similar to those reported in other FLCs [4,6]. As we can rewrite $\Delta\varepsilon_3$ as $-(P_S/\theta)^4/(\theta^2 q_0^6)$ except the numerical factor and the values of P_S/θ and $1/q_0$ reach finite ones at T_C

[2], $\Delta\varepsilon_3$ is expected to diverge with a negative sign at T_C in the Sm-C^* phase. We could not determine T_C exactly by dielectric measurement, but we can regard it 55.0 °C from the divergent behavior of $\Delta\varepsilon_3$. The steep decrease of $\Delta\varepsilon_3$ above 55.0 °C is due to the contribution of the soft mode in the Sm-A phase [13]. Strictly speaking, the profile of ε_3^* calculated for the soft mode [16] is slightly different from Eq. (6), but the spectra above 55.0 °C have been accidentally fitted well by Eq. (6).

Finally, we would like to discuss the material constants of FLCs evaluated from the best-fitted parameters of the nonlinear dielectric relaxation spectra. By combining Eqs. (5) and (6) and $\tau=\gamma/Kq_0^2$, we can calculate the values of P_S, γ, and Kq_0^2 from the best-fitted values of $\Delta\varepsilon_1$, $\Delta\varepsilon_3$, and τ as

$$P_S=\left(-\frac{3\Delta\varepsilon_1^3}{2\Delta\varepsilon_3}\right)^{1/2}. \tag{9}$$

$$\gamma=-\frac{3\Delta\varepsilon_1^2\tau}{4\Delta\varepsilon_3}\frac{F}{E}, \tag{10}$$

$$Kq_0^2=-\frac{3\Delta\varepsilon_1^2}{4\Delta\varepsilon_3}\frac{F}{E}. \tag{11}$$

In Eqs. (9)–(11), we regard the local field F as the electric field working on FLCs in a bulk instead of E. As the linear permittivity of CS1017 is rather large, we can approximately use the value of $F/E=1.5$ in Eqs. (10) and (11). The temperature dependence of P_S, γ, and Kq_0^2 calculated by Eqs. (9)–(11) are respectively shown in Fig. 4. In Fig. 4(a), the values of P_S directly measured by the triangular wave method [18] are plotted as open circles for comparison. The difference between them is found to be small except near the phase transition temperature. This discrepancy is partially due to the neglect of the contribution from the soft mode and the insufficient assumption of the local field for third-order nonlinear response. If the helical pitch $2\pi/q_0$ and tilt angle θ are known, we can also evaluate the elastic constant K_3 from the values of Kq_0^2. By using the measured values of $q_0=4.7\,\mu\mathrm{m}^{-1}$ and $\theta=18°$ at 50 °C, we can obtain $K_3=6.9$ pN, which is comparable to the values of K_3 for nematic liquid crystals.

In summary, we have studied the nonlinear dielectric relaxation spectra of FLCs experimentally and analyzed them theoretically by the simple torque balance equation. We have also calculated the material constants of FLCs from the obtained parameters of spectra to check the effectiveness of our analysis quantitatively and found that our analysis remains semiquantitative. To improve our theoretical treatment, we need to take into account the fluctuation of magnitude of the tilt angle and calculate with the extended mean-field model which was used for the analysis of the linear spectrum [5]. We also need to know the exact expression of the local field for the nonlinear response.

This work is supported by Grant-in-Aid for Scientific Research from the Ministry of Education, Science, Sports and Culture of Japan. The authors also thank Chisso Co., Ltd. for supplying the FLC sample.

[1] R. B. Meyer, L. Liebert, L. Strzelecki, and P. Keller, J. Phys. (France) **36**, L69 (1975).
[2] B. Žekš and R. Blinc, *Ferroelectric Liquid Crystals, Principles, Properties and Applications* (Gordon and Breach, Philadelphia, 1991), Chap. 5.
[3] R. Blinc and B. Žekš, Phys. Rev. A **18**, 740 (1978).
[4] A. Levstik, T. Carlsson, C. Filipič, I. Levstik, and B. Žekš, Phys. Rev. A **35**, 3527 (1987).
[5] T. Carlsson, B. Žekš, C. Filipič, and A. Levstik, Phys. Rev. A **42**, 877 (1990).
[6] A. Levstik, Z. Kutnjak, C. Filipič, I. Levstik, Z. Bregar, B. Žekš, and T. Carlsson, Phys. Rev. A **42**, 2204 (1990).
[7] L. Benguigui, J. Phys. (France) **43**, 915 (1982).
[8] K. Yoshino, M. Ozaki, T. Sakurai, K. Sakamoto, and M. Honma, Jpn. J. Appl. Phys. **23**, L175 (1984).
[9] S. Ikeda, H. Kominami, K. Koyama, and Y. Wada, J. Appl. Phys. **27**, 3339 (1987).
[10] T. Furukawa, M. Tada, K. Nakajima, and I. Seo, Jpn. J. Appl. Phys. **27**, 200 (1988).
[11] T. Furukawa and K. Matsumoto, Jpn. J. Appl. Phys. **31**, 840 (1992).
[12] Y. Kimura and R. Hayakawa, Jpn. J. Appl. Phys. **32**, 4571 (1993).
[13] Y. Kimura and R. Hayakawa, Mol. Cryst. Liq. Cryst. Sci. Technol., Sect. A **261**, 225 (1995).
[14] Y. Kimura, R. Hayakawa, N. Okabe, and Y. Suzuki, Phys. Rev. E **53**, 6080 (1996).
[15] Y. Kimura and R. Hayakawa, *Abstracts of the 16th Japanese Liquid Crystal Conference* (Chemical Society of Japan, Tokyo, 1990), Vol. 160.
[16] H. Orihara and Y. Ishibashi, J. Phys. Soc. Jpn. **62**, 489 (1992).
[17] Y. Kimura and R. Hayakawa, Jpn. J. Appl. Phys. **31**, 3387 (1992).
[18] K. Miyasato, S. Abe, H. Takezoe, A. Fukuda, and E. Kuze, Jpn. J. Appl. Phys. **22**, L661 (1983).